Cellulose (2021) 28:9837–9855
https://doi.org/10.1007/s10570-021-04148-3

ORIGINAL RESEARCH

Phosphorylated hazelnut shell waste for sustainable lithium recovery application as biosorbent

Yaşar Kemal Recepoğlu · Aslı Yüksel

Received: 27 January 2021 / Accepted: 13 August 2021 / Published online: 19 August 2021

Abstract Hazelnut shell waste was phosphorylated to develop a novel biosorbent based on natural renewable resource for the recovery of lithium from aqueous solution. For the synthesized biosorbent, the surface morphology and mapping by SEM–EDS, chemical properties by FTIR, elemental analysis by XPS, specific surface area by BET, crystallinity by XRD and thermal properties by TGA were elucidated elaborately. The influence of biosorbent dosage, initial concentration, temperature, contact time, pH and coexisting ions were investigated. The equilibrium sorption capacity reached 6.03 mg/g under optimal conditions (i.e., biosorbent dosage of 12.0 g/L, initial Li concentration of 100 mg/L, pH value of 5.8, sorption temperature of 25 °C, and sorption time of 6 min). According to the sorption behavior of the phosphorylated hazelnut shell waste the Freundlich model proved to be more suitable than the Langmuir model indicating maximum sorption capacity as 7.71 mg/g at 25 °C. Thermodynamic parameters obtained by different isokinetic temperatures disclosed that the ion exchange reaction was feasible, spontaneous, and exothermic where the interaction between biosorbent surface and solvent plays an important role. A preliminary test on the Li recovery from geothermal water was also performed to check its applicability in a real brine. Desorption studies at 25 °C revealed that relatively higher desorption efficiency and capacity were achieved at 97.4% and 5.93 mg/g, respectively with a 1.0 M H_2SO_4 among other regenerants (i.e., HCl and NaCl). Concentrations of Li and the other cations were determined via ICP-OES. Due to such outstanding features, the novel phosphorylated hazelnut shell waste had great potential for lithium recovery from aqueous solution by being added value as a waste and recovering a strategic element of modern life simultaneously.

Supplementary Information The online version contains supplementary material available at https://doi.org/10.1007/s10570-021-04148-3.

Y. K. Recepoğlu · A. Yüksel (✉)
Department of Chemical Engineering, Izmir Institute of Technology, Urla, 35430 Izmir, Turkey
e-mail: asliyuksel@iyte.edu.tr

A. Yüksel
Geothermal Energy Research and Application Center, Izmir Institute of Technology, Urla, Izmir, Turkey

Graphic abstract

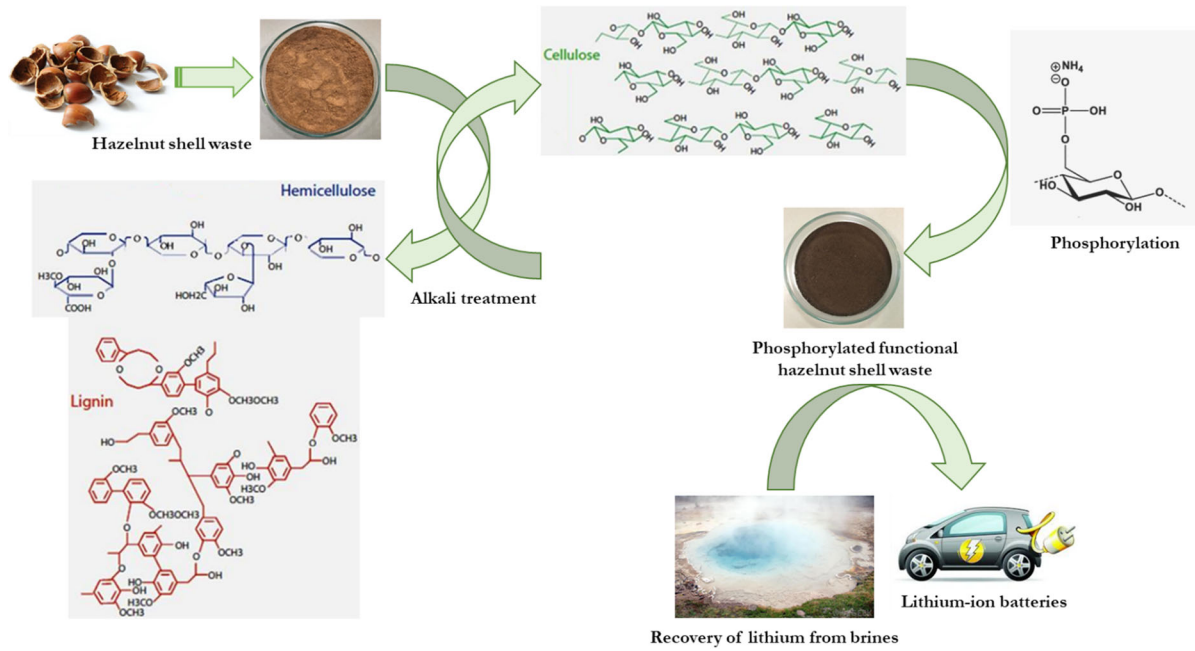

Keywords Biomass · Biosorbent · Hazelnut shell · Lithium · Phosphorylation

Introduction

A million tons of waste and by-products are produced by modern agricultural facilities every year that have potential as useful resources (Sarker et al. 2017). These agro-industrial residues obtained from harvesting and industrial processing of agricultural crops can be a promising alternative to traditional adsorbents, since they are readily available, cheap, highly sorptive and easily modifiable (Ngo et al. 2015). A plenty of agricultural wastes which have lignocellulosic structures such as peanut shell (Witek-Krowiak et al. 2011), walnut shell (Segovia-Sandoval et al. 2018), cotton stalk/wheat stalk (Xu et al. 2011), rice husk (Chuah et al. 2005), orange peels (Romero-Cano et al. 2016), sugar cane bagasse and olive stones (Moubarik and Grimi 2015) have been extensively modified and used for bioremediation particularly in heavy metal and textile dye removal from water. Recently, hazelnut processing plant wastes, hazelnut shell and hazelnut skin, were used without further chemical modification for the simultaneous removal of multi-elements (Al, As, Cd, Cr, Cu, Fe and Pb) from water (Özlem 2019).

One of lignocellulosic biomass, hazelnut, is an agricultural product grown in significant quantities in Turkey due to its climatological and ecological conditions and land property. Therefore, Turkey is the leader in the production of shelled hazelnuts (*Corylus Avellana L.*) in the world by supplying namely, 70% of the total production (650,000 tons/year), followed by Italy (13%), the USA (4%), Azerbaijan (3%), Spain (3%) and Georgia (3%) in 2017 with a huge gap in terms of the production capacity as shown in Fig. S1 (Alasalvar et al. 2009; Guney 2013). It has been reported that 70 wt% of the product is shell and pruning waste is produced as 2.7 times of the product after harvesting (Alkaya et al. 2010). Although hazelnut shell found use in plywood, linoleum and paint industry in the USA, Italy, and Germany, which have advanced technologies, it is mostly used for heating purposes as hazelnut coals in Turkey. Currently, hazelnut bark and pruning wastes are used as fuel, while the slag is left in the soil as a fertilizer or directly burned after the harvest (Çöpür et al. 2008; Özlem 2019; Şenol 2019). Considering

those wastes arising out of high production rate, converting such a large amount of lignocellulosic material into valuable products instead of low value applications is of great importance for our country's economy and environment. Over the last decade, sustainability and green chemistry has been important for the development of the next generation of materials in which the use of bio-based polymer matrices might allow the reduction of environmental impacts by using renewable carbon and by achieving more easily biodegradable or reusable materials (Illy et al. 2015). Among several strategies for the modification of biomass, introduction of phosphorous moieties to bio-based compounds have been widely studied due to their fire resistance, excellent chelating, and metal-adhesion properties. The grafting reaction of phosphorus compounds to cellulose can undergo in several routes: with tervalent (III) or pentavalent (V) phosphorus reagents, by direct or indirect bonding of phosphorus functions to cellulose, using cellulose or cellulose derivatives as substrates, with or without catalysts, in heterogeneous or homogeneous reaction environment, etc. Although phosphorus derivatives such as $POCl_3$, H_3PO_4 and P_2O_5 are the most common phosphorylating agents for pentavalent phosphorus, these reagents, usually leading to anionic cellulose phosphates, show a lower esterification reactivity than the similar derivatives of trivalent phosphorus and cause a higher degradation of the cellulose substrate. This drawback is partially overcome if urea is introduced in the phosphorylation system as a catalyst (Shi et al. 2014; Illy et al. 2015; Kokol et al. 2015). On the other hand, lignocellulosic biomasses are rich in polysaccharides (cellulose and hemicellulose) and lignin. Before going through the modification hemicellulose and lignin should be removed from the lignocellulose that inhibit cellulose utilization in the biomass. A range of chemical, physical, physicochemical, and biological pretreatment techniques have been developed to improve the accessibility to cellulosic fibers in the biomass. Among these methods alkaline pretreatment is widely preferred for the delignification (removal of lignin) of lignocellulosic biomass which enhances the reactivity of the remaining carbohydrates. NaOH pretreatment of several lignocellulosic materials has been reported to increase the processability of the biomass by decreasing the degree of polymerization, increasing the surface area and cutting down on lignin content (Hoşgün and Bozan 2019). Moreover, the NaOH treatment specifically breaks the van der Waals and hydrogen bonds between cellulose molecules and brings about more hydroxy groups to become exposed to H_3PO_4 in the second step of the process that activates hydroxy groups in cellulosic portion of hazelnut shell waste before undergoing phosphorylation reaction (Illy et al. 2015).

The main scope of this study is to obtain low cost biosorbent from waste biomass for the recovery of lithium by attaching phosphoric functional groups as lithium is the strategic element of the twenty-first century. To meet the dramatic rise in the global lithium consumption due to the steep increase in the use of electric vehicles and mobile electronics, the attention has been turned to search for alternative lithium sources (Kim et al. 2019). Because a shortage of lithium is expected soon due to an uneven global distribution of lithium reserves as demand for lithium soars (Grosjean et al. 2012). Biosorption is highly effective in separation of organic and inorganic substances in soluble or insoluble forms from an aqueous solution through the utilization of low-cost biosorbent materials among other methods (Fomina and Gadd 2014). Most of the studies on lithium recovery from a mixture of diverse cations with high concentrations have been conducted by inorganic adsorbents such as $H_4Mn_5O_{12}$ nanotubes lithium ion sieve (Xu et al. 2019), iron-doped lithium titanium oxides (Wang et al. 2018), titanium type ion sieve (H_xTiO_3) (Wang et al. 2017), λ-MnO_2 (Yoshizuka et al. 2002; Kitajou et al. 2006; Park et al. 2012; Recepoğlu et al. 2017, 2018). To our best knowledge, no studies have been found in the literature regarding the synthesis of lithium sorption-capable biosorbents from lignocellulosic wastes. In this context, the reaction of cellulose with phosphorous acid in molten urea by Inagaki et al. (1976) and Suflet et al. (2006) were pioneered the synthesis and characterization of phosphorylated hazelnut shell waste. By doing this, hazelnut shell waste, which is a real cellulose resource, cheap, abundant, and easily accessible in Turkey was evaluated properly by adding a value to a waste and used for the recovery of lithium from aqueous solution simultaneously. Moreover, the spent biosorbent can be converted into a fertilizer under suitable conditions via pyrolysis since it contains phosphorous and nitrogen as further use. In this way, the further use of this bio-

sorbent for adsorption–desorption of Li is environmentally friendly and cost-effective.

Experimental

Materials

Hazelnut shell wastes as biomass used in this study were supplied from Ordu province, Turkey where hazelnut trees were commonly cultivated. Before using, they were washed extensively with tap water to remove the dust and soil, sprayed with distilled water, and dried in an oven at 60 °C. After that, they were ground into small pieces by a laboratory type grinder and sieved. Samples having particle size range of 150–300 μm were phosphorylated. The characteristics of hazelnut shell as proximate, structural and ultimate analysis identified in the previous study (Gozaydin and Yuksel 2017) are given in Table S1.

Di-Ammonium hydrogen phosphate, hydrochloric acid (37%), lithium chloride, ortho-phosphoric acid (85%), potassium chloride, sodium chloride, sodium hydroxide, sulfuric acid (95–97%) and urea were purchased from Merck.

Methods

Synthesis of the biosorbent

High alkali treatment of hazelnut shell waste The procedure applied is given as follows:

(1) 10 g of hazelnut shell waste was added into 10 M NaOH solution (100 mL) and the mixture was stirred at room temperature (25 °C) for 2 h.
(2) Then, to precipitate hazelnut shell waste dissolved in the alkali solution, 10 M HCl (100 mL) was added to the mixture.
(3) Next, the mixture was washed with excess water and filtered to remove the alkaline.
(4) Finally, the residue dried at 70 °C for 6 h was ground using coffee grinder.

Chemical modification of hazelnut shell waste (Phosphorylation reaction) Chemical modification of hazelnut shell waste for attaching phosphorous functional groups to its cellulosic constituents was carried out based on the patent proposed by Yabusaki (2010) as follows:

(1) 0.15 mol phosphoric acid, 0.2 mol diammonium hydrogen phosphate and 1 mol urea was dissolved in 150 mL water to prepare the phosphorylating chemical solution.
(2) Then, 10 g previously NaOH treated hazelnut shell waste was added into this solution and thoroughly mixed.
(3) Next, the mixture was left at room temperature (25 °C) for 1 h before its water content was evaporated and the residue was completely dried at 105 °C for 18 h.
(4) After that, the mixture was heated to 150 °C and it was left to react at this temperature for 2 h.
(5) Finally, the reaction product was washed with excess water and dried at 70 °C for 6 h. The solid product was ground using a coffee grinder to give phosphorylated functional hazelnut shell waste as biosorbent (Fig. S2 (b)).

Characterization of the synthesized biosorbent The photomicrography was obtained using Scanning Electron Microscopy (Quanta 250 SEM) by coating free surfaces of the materials with thin layers of gold (Emitech K550X) at an accelerating voltage range of 3.0–5.0 kV. The chemical compositions of pristine and modified materials were determined by Energy Dispersive Spectrometer (EDS) combined with SEM.

Fourier Transform Infrared Analysis (FTIR) was conducted on FTIR-8400S spectrophotometer (Shimadzu, Japan) to provide insights into the structure change between pristine and modified hazelnut shell wastes. Infrared spectra were recorded over a wavenumber range from 400 to 4000 cm^{-1}. A total of 24 scans was averaged at a resolution of 4 cm^{-1}.

Quantitative elemental analysis was performed by XPS (Thermo Scientific, Nexsa) having 180° hemispherical analyzer-128 channel detector for C, O, P, N and Li elements based on the change in the bond energies in the molecule. The elements were scanned in the range of 0.0–1350.0 eV using monochromatic Al Kα X-rays (1486.68 eV) with a pass energy of 30 eV and scan number of 3.

The BET surface area, pore size and pore size distribution were measured using a surface area and porosity analyzer (Micromeritics Gemini V) equipped

with Micromeritics VacPrep 061 Sample Degas System using N_2-adsorption technique.

XRD measurements were taken with Philips X'Pert Pro equipment using Cu-Kα radiation as X-ray source having generator voltage of 45 kV and tube current of 40 mA. Scanning was done in the range of $10° < 2\theta < 30°$ with a wavelength of 1.54 A°.

The measurable differences in the heat capacity and thermal stability of pristine and phosphorylated materials were determined by TGA equipment (Setaram). Thermograms were obtained by heating the samples from 30 to 1000 °C in a dynamic heating regime under nitrogen with a constant heating rate of 5 °C/min.

Lithium sorption experiments

The sorbent dosage experiments were performed by mixing various amounts (0.1–0.5 g) of phosphorylated hazelnut shell waste with 25 mL of LiCl test solution (Li^+: 10 mg/L) in plastic bottles and shaking in a shaker (Grant OLS200) at 25 °C, 180 rpm. To investigate the effects of initial solution concentration and temperature on sorption performance, various initial concentrations, ranging from 10 to 100 mg/L and various temperatures (25–45 °C) were carried out with a constant mass of phosphorylated functional hazelnut shell waste (0.35 g). In addition, pH effect was studied using 10 mg/L of Li^+ solution having different pH values ranging from 2 to 8. The effect of contact time was observed by sorption kinetics experiment at specified time interval (0–60 min) and the effect of competitive ions was studied by adding Li^+, K^+, Na^+, Ca^{2+} and Mg^{2+} (10 mg/L) at ambient temperature as well. The corresponding Li^+ and the other ion concentrations were determined using an ICP-OES instrument (Agilent Technologies, 5110). All the experiments were repeated twice, and average values were reported with error bars as standard deviation.

The sorption capacity and recovery percentage of Li were calculated by the following equations, respectively:

$$q_e = \frac{(C_0 - C_e)V}{m} \quad (1)$$

$$R = \frac{C_0 - C_e}{C_0} \times 100 \quad (2)$$

where q_e. is the unit sorption capacity at equilibrium (mg/g), R is the recovery percentage of Li, C_0 and C_e are the initial Li concentration (mg/L) and Li concentration at equilibrium (mg/L), respectively. V is the volume of Li solution (L), and m is the dry weight of biosorbent (g).

Freundlich, Langmuir and Temkin isotherm models were used to analyze the sorption behavior of the synthesized biosorbent. The Langmuir model (1916) is expressed as follows:

$$q_e = \frac{Q_{max} K_L C_e}{1 + K_L C_e} \quad (3)$$

where Q_{max} (mg/g) is the maximum sorption capacity and K_L (L/mg) is the Langmuir constant related to the affinity of the binding sites.

The Freundlich model (1907) is given as follows:

$$q_e = K_F C_e^{1/n} \quad (4)$$

where K_F ((mg/g) $(L/mg)^{1/n}$) and n are Freundlich constants for sorption capacity and sorption intensity of the biosorbent, respectively.

Temkin model (Tempkin and Pyzhev 1940) is described as follows:

$$q_e = (RT/b_T) ln(AC_e) \quad (5)$$

where $B = RT/b_T$, which is the Temkin constant related to heat of sorption whereas A (L/mg) is the equilibrium binding constant related to the maximum binding energy. R (8.314 J/mol K) is the universal gas constant and T (K) is the absolute solution temperature.

Desorption and regeneration of the phosphorylated functional hazelnut shell waste

Li was desorbed from saturated biosorbent by sorption experiment via 100 mg L^{-1} Li^+ and 12 g/L biosorbent dosage using 0.25 M, 0.5 M, and 1.0 M of NaCl, HCl and H_2SO_4 as eluents. After regeneration, concentrated Li can be recovered by evaporation of spent solution in Li salt forms and further purification steps can be considered.

Results and discussion

Characteristics of the biosorbent

SEM and EDS analysis

The surface morphologies of the samples at 5000 times magnification are shown in Fig. 1. While the surfaces of both pristine hazelnut shell waste (Fig. 1a) and NaOH treated one (Fig. 1b) in powdery form were smoother with less burrs on the surface, the surface of phosphorylated hazelnut shell (Fig. 1c) became folded and rough that can be attributed to the phosphorylation reaction of active hydroxy groups in pristine hazelnut shell waste. In addition, several small particles seen on the surface of phosphorylated hazelnut shell waste and between layers suggested that the phosphoric functional group associated with the pristine material successfully. Furthermore, spots appeared on phosphorylated hazelnut shell confirmed its specific surface area having active biosorption sites for Li to be attached from aqueous solutions. Figure 1d was the apparent morphology of Li-loaded phosphorylated hazelnut shell waste. Compared with phosphorylated hazelnut shell waste before biosorption, the surface of its Li-loaded form had more irregularity and the fibrous structure was more obvious. That could be explained by the fact that H^+ ions in the phoshporous functional group were exchanged by Li^+ ions in the aqueous solution hence reductive spots have appeared on Li-loaded phosphorylated hazelnut shell waste in acid medium. This difference can also be clearly distinguished in SEM images at 10,000 times maginification given in Fig. S3.

Elemental mapping and energy dispersive spectra of phosphorylated hazelnut shell waste are shown in Fig.'s 1(e) and 1(f). Highly exposed phosphoric functional group were well distributed in the cellulosic portion of the hazelnut shell waste as revealed by P EDS map (Fig. 1e). The peaks pertained to phosphorylated hazelnut shell waste regarding precise elemental composition of its surface from EDS analysis gives C (41.98 wt%), O (40.70 wt%), N (11.66 wt%) and P (5.67 wt%). Although carbon, oxygen and nitrogen contribute most to the elemental composition of the synthesized biosorbent, which is attributed to the organic nature of lignocellulosic residues, the considerable presence of phoshorous element suggests that the high exposure of phosporic groups on the surface of the cellulosic portion of hazelnut shell waste.

Fig. 1 SEM surface morphology (magnification 5,000x): ▶ **a** pristine hazelnut shell waste, **b** NaOH treated hazelnut shell waste, **c** phosphorylated hazelnut shell waste and **d** lithium-loaded phosphorylated hazelnut shell waste **e** C, O, N and P elemental mapping for phosphorylated hazelnut shell waste, **f** EDS results

FTIR analysis

The micro-FTIR spectra of the pristine hazelnut shell and phosphorylated hazelnut shell waste are shown in Fig. 2a. After phosphorylation of hazelnut shell, a peak at wave number 1039 cm^{-1} in the phosphorylated hazelnut shell was found that corresponded to the characteristic absorption peak of a P–O stretching vibration belonging a medium to strong wide band at 1040–910 cm^{-1} for the compounds containing P–OH group. Moreover, the bands at 823 cm^{-1} and 922 cm^{-1} were attributed to the P–O–P symmetric and antisymmetric stretching vibrations, respectively. For the phosphorylated hazelnut shell, a new peak at 1238 cm^{-1} appeared that was assigned to the strong P=O bond. Absorbance of the peak at 1315 cm^{-1} ascribed to CH_2 coupled with OH deformation disappeared due to the phosphorylation of hydroxyl groups (Shi et al. 2014). The peak around 1402 cm^{-1} presents weak –OH acid group so that the OH stretching vibration band became more asymmetric owing to introduction of more acidic OH groups of phosphoric acids into the polymer in the range 3200–3600 cm^{-1} (Socrates 2004; Luneva and Ezovitova 2014). Micro-FTIR results confirmed a successful synthesis of phosphorylated functional biosorbent from hazelnut shell waste.

XPS analysis

XPS is another useful technique to analyze and confirm the functional groups on surface of materials semi-quantitatively. Broad scan XPS patterns of the pristine, phosphorylated and Li-loaded phosphorylated hazelnut shell are shown in Fig. 2b. For the pristine hazelnut shell, only characteristics peaks of C 1 s, N 1 s and O 1 s could be observed in XPS at 285 eV, 400 eV and 533 eV, respectively. In contrast,

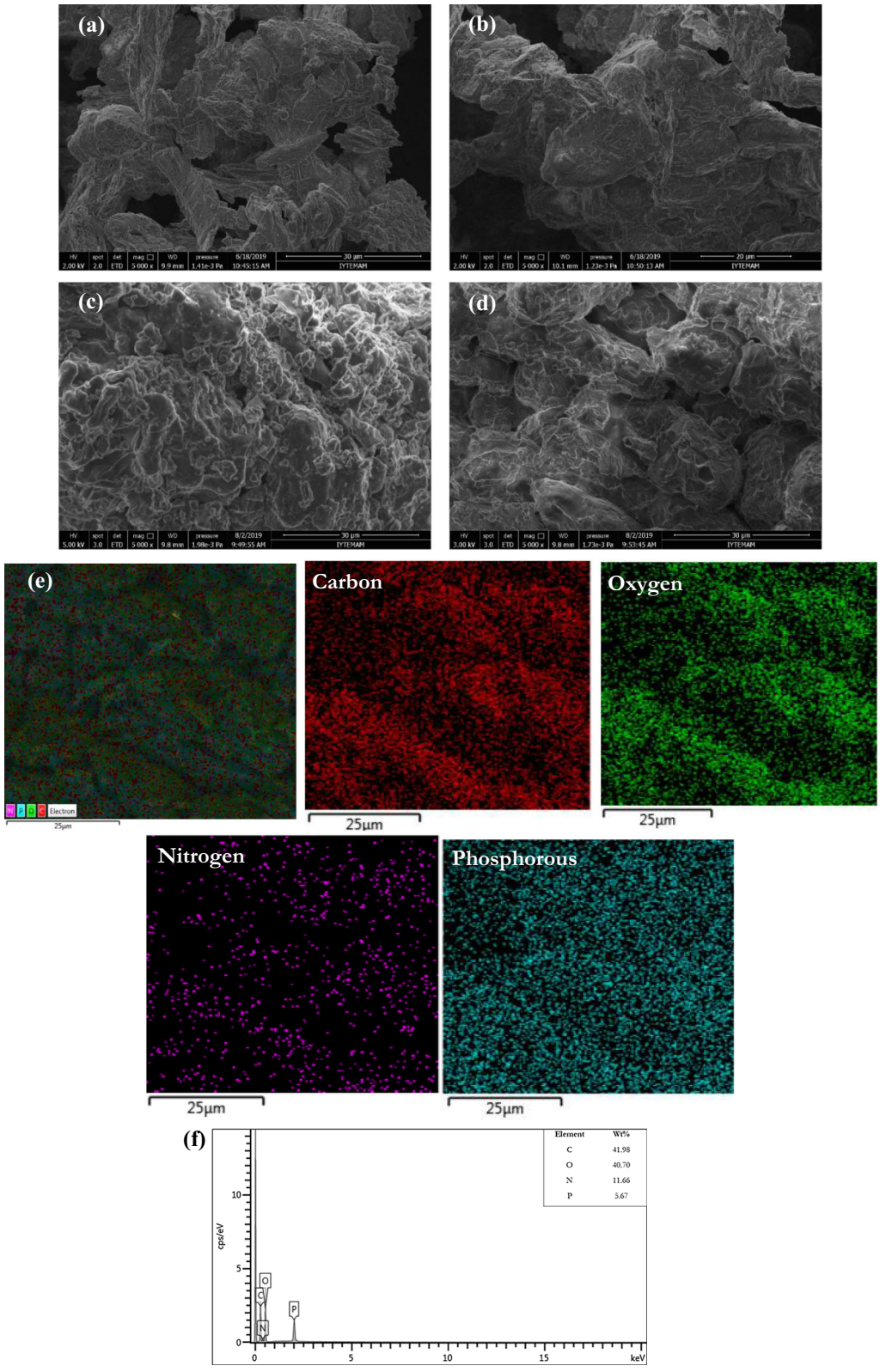
(a)
(b)
(c)
(d)
(e)
Carbon
Oxygen
Nitrogen
Phosphorous
25µm
(f)
Element Wt%
C 41.98
O 40.70
N 11.66
P 5.67
cps/eV
keV

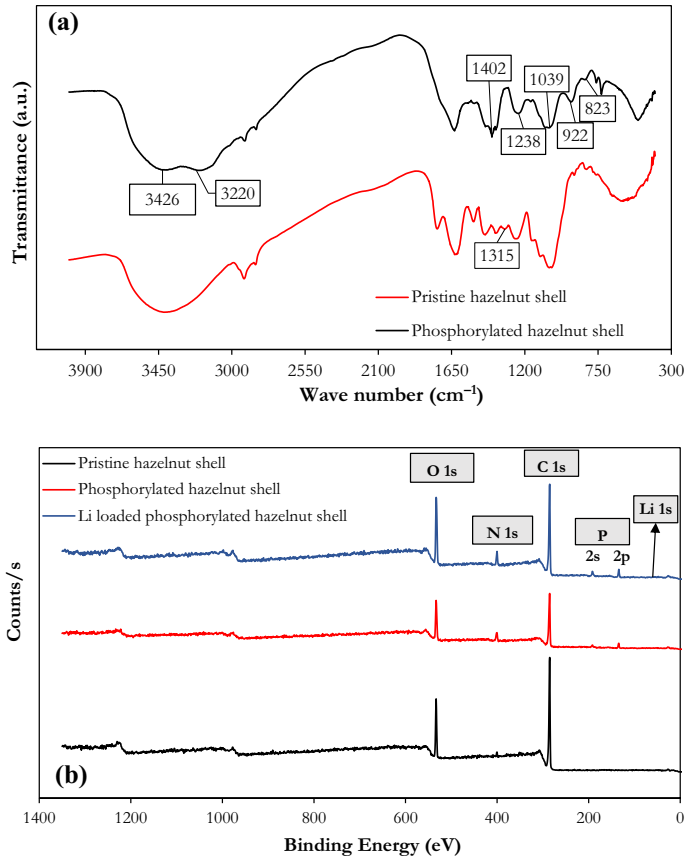

Fig. 2 **a** Micro-FTIR spectra of both pristine and phosphorylated hazelnut shell waste **b** XPS diagram of pristine, phosphorylated and Li-loaded phosphorylated hazelnut shell waste

after phosphorylation, new peaks of P 2 s and P 2p at 190 eV and 134 eV, respectively, appeared for the phosphorylated hazelnut shell and it further identified the successful phosphorylation that agreed well with the micro-FTIR results. Although the detection of lithium is difficult due to the low photon energy of this element which emits low energy peaks close to the electronic noise of the detection system, large number (50) of scans were done to acquire Li 1 s spectrum for the Li-loaded phosphorylated hazelnut shell. Hence, the signal observed at 55 eV was attributed to binding energy of Li 1 s which could be better determined by high resolution XPS spectra given in Fig. S4.

The atomic concentrations of all present elements for pristine, phosphorylated and Li-loaded phosphorylated hazelnut shell are listed in Table 1. After NaOH treatment ca. 4% increase in O and ca. 4% decrease in C content were observed due to removal another carbonaceous portion of the biomass. Phosphorylated hazelnut shell after grafting of phosphorous group contains 3.27% P in the surface. Data confirmed that phosphorylation occurred preferentially at the surface where the hydroxyl functional groups are more accessible. In addition, the O 1 s peak for modified hazelnut shell showed an increase in intensity and a slight chemical shift to a higher BE value compared to unmodified hazelnut shell corresponding to 17.89% and 21.32% of O content, respectively. These changes can be attributed to non-bridging oxygen in the phosphate group (O=P) and oxygen double bonded to carbon (O=C) from carbamates. It seemed that the O=P bond was responsible for O 1 s evolution since the carbamate moiety came from the less favored side reaction between cellulose and urea. N content increased from 3.24 to 9.49% after phosphorylation of hazelnut shell which assigned to nitrogen covalent bonds in the carbamate moiety (N–C=O and NH_2) in the surface. 5.95% Li proved lithium sorption capability of phosphorylated hazelnut shell.

Table 1 Surface composition (atom fraction, %) of pristine, NaOH treated, phosphorylated and Li-loaded phosphorylated hazelnut shell wastes

Elements	Pristine hazelnut shell (atom fraction, %)	NaOH treated hazelnut shell (atom fraction, %)	Phosphorylated hazelnut shell (atom fraction, %)	Li-loaded phosphorylated hazelnut shell (atom fraction, %)
C 1 s	78.92	74.51	65.93	62.27
O 1 s	17.86	22.32	21.32	21.57
N 1 s	3.24	3.19	9.49	6.50
P 2p	–	–	3.27	3.72
Li 1 s	–	–	–	5.95

BET analysis

BET surface areas and pore structures of pristine (PHS), NaOH treated (NHS) and phosphorylated functional hazelnut shell waste (FHS) are provided in Table 2. It was found that the NaOH treatment increased BET surface area threefold and total pore volume fivefold due to removal of lignin that is also a barrier to access the cellulose. However, further phosphorylation process decreased the BET surface areas and the pore volumes of NHS as intermediate due to the blockage of internal porosity by incorporated phosphorous functional group. In addition, the percentage of micropore of sample decreased from $\sim$ 8 to $\sim$ 3% and macropore increased from $\sim$ 50 to 70% at the end of total modification, thus the micropores might have been enlarged and converted into macropores leading to a decrease in specific surface area. Moreover, the total pore volume was also greatly reduced after phosphorylation.

XRD analysis

The X-ray diffractograms of pristine, NaOH treated and functionalized hazelnut shell waste samples are shown in Fig. 3. In general, the diffractogram characteristic of hazelnut shell waste showed cellulose identifier as strongly justified by the presence of a peak at 2θ angle values around 16.5° and 22.6° whose patterns look similar to those from amorphous samples reported in the literature (Poletto et al. 2012; French and Santiago Cintrón 2013; French 2020). Cellulose is composed of glucose monomer units in the form of linear chains making up the crystalline structure that is essentially attributed to hydrogen bonding interactions and Van der Waals forces among adjacent molecules (Tomul et al. 2019). In contrast, hemicellulose (with branched as well as straight polymer chains) and lignin (with three-dimensional polymer) are amorphous (Cagnon et al. 2009).

Crystallinity index (CrI %) values were calculated by using Segal equation (Eq. (6)) (Segal et al. 1959; French 2014):

Table 2 Pore size analysis, BET surface area and crystallinity index value of pristine hazelnut shell waste, NaOH treated hazelnut shell waste and phosphorylated functional hazelnut shell waste

Material	Pore volume (%)			Total pore volume (cm^3/g)	BET Surface Area (m^2/g)	CrI (%)
	Micropore (< 2 nm)	Mesopore (2–50 nm)	Macropore (> 50 nm)			
*PHS	7.89	42.00	50.11	0.001407	1.7367	19.76
**NHS	4.07	21.04	74.89	0.007496	5.6877	27.55
***FHS	3.30	27.00	69.70	0.000637	0.8193	17.88

*PHS: Pristine hazelnut shell waste

**NHS: NaOH treated hazelnut shell waste

***FHS: Phosphorylated functional hazelnut shell waste

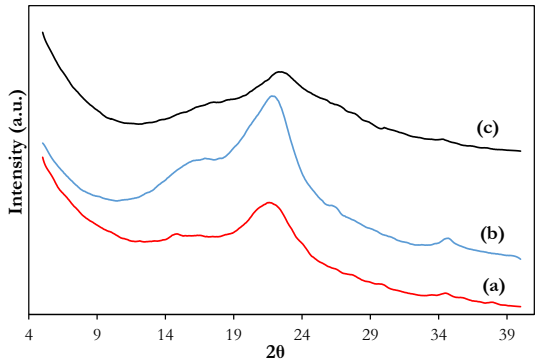

Fig. 3 X-ray diffraction patterns of **a** pristine, **b** NaOH treated and **c** phosphorylated functional hazelnut shell waste

$$CrI(\%) = \frac{I_{200} - I_{am}}{I_{200}} \times 100 \quad (6)$$

where *CrI* is the relative degree of crystallinity, I_{200} is the maximum intensity (in arbitrary units) of the 200 lattice diffraction and I_{am} is the intensity of diffraction in the same units at 2θ = 18°. The calculated CrI % values are given in Table 2. After pretreatment by NaOH crystallinity index increased from 19.76 to 27.55% as expected since amorphous contributors i.e., hemicellulose and lignin were removed. However, then crystallinity index decreased to 17.88% because modification by phosphorylation led to the diffraction peak located at 200 lattice plane becomes flatter, also indicating a decrease in crystallinity. Nonetheless, it was believed that the improved crystallinity of cellulose increases its rigidity, which can lead to increase the mechanical properties (higher tensile strength) of cellulose based composite.

TGA analysis

Figure 4 illustrates thermal profiles of pristine, NaOH treated and phosphorylated functional hazelnut shell waste by pyrolysis. As pronounced in the differential thermogravimetric curve (DTG) of pristine hazelnut shell waste (Fig. 4a) three peaks at 70 °C, 260 °C and 338 °C were observed corresponding to moisture evaporation, hemicellulose, and cellulose thermal decomposition, respectively. Specifically, a minor weight loss of 5% at 70 °C seen in the thermogravimetric analysis (TGA) curve is explained with the adsorbed and bound water molecules. In addition, thermal biomass degradation of hemicellulose and cellulose occurred by 9.36% weight loss and 30.07% weight loss due to decomposition of glycosidic bonds (C–O–C). Meanwhile, lignin decomposition could not be observed since the lignin is commonly known as the most difficult main structural component in the biomass for thermal decomposition (often ranging from 160 °C to elevated temperatures) (Tran et al. 2017). The complete carbonization of hazelnut shell waste required the minimum temperature of 363 °C and at the final decomposition temperature in the studied temperature range, i.e. 1000 °C, only 25% of the char remained.

Compared to the unmodified pristine hazelnut shell waste, an almost similar nature of degradation curve (Fig. 4b) with microcrystalline cellulose, having the onset of degradation at 285 °C and with the degradation peak around 330 °C (Das et al. 2010) was obtained for NaOH treated hazelnut shell waste. Since alkali pretreatment was applied to remove lignin and a part of the hemicellulose, this result was in line with the literature (Kim et al. 2016).

On the other hand, the thermal analysis of the phosphorylated functional hazelnut shell waste indicated a relatively complex pyrolysis process (Fig. 4c) since the grafting of phosphorous groups on the surface of cellulose particles modifies the thermal degradation pathway of cellulose by decreasing its onset degradation temperature and by improving the formation of high amount of char residues (Costes et al. 2016). A similar minor weight loss (ca. 7%) was observed at 73.5 °C due to evaporation of water molecules adsorbed on the phosphorylated functionalized hazelnut shell waste. Thereafter, the initial prominent major weight loss by 18.7% was at 200–250 °C, and it verified that the phosphorous groups increased the thermal decomposition reaction of the cellulosic polymer (and hence the heat resistance of the material was reduced), but the carbonization (and hence the flame resistance) increased significantly instead. The final observed peak at 828 °C with another major weight loss of 26.27% indicates that the phosphorous functional group was decomposed. It is widely known in the literature that cellulosic materials containing phosphorous group have flame retardant properties (Aoki and Nishio 2010; Ghanadpour et al. 2015; Rol et al. 2019). At the final decomposition temperature (1000 °C) of the phosphorylated functional hazelnut shell waste the char residue was 33% which is in good agreement with the improvement in the char formation after phosphorylation.

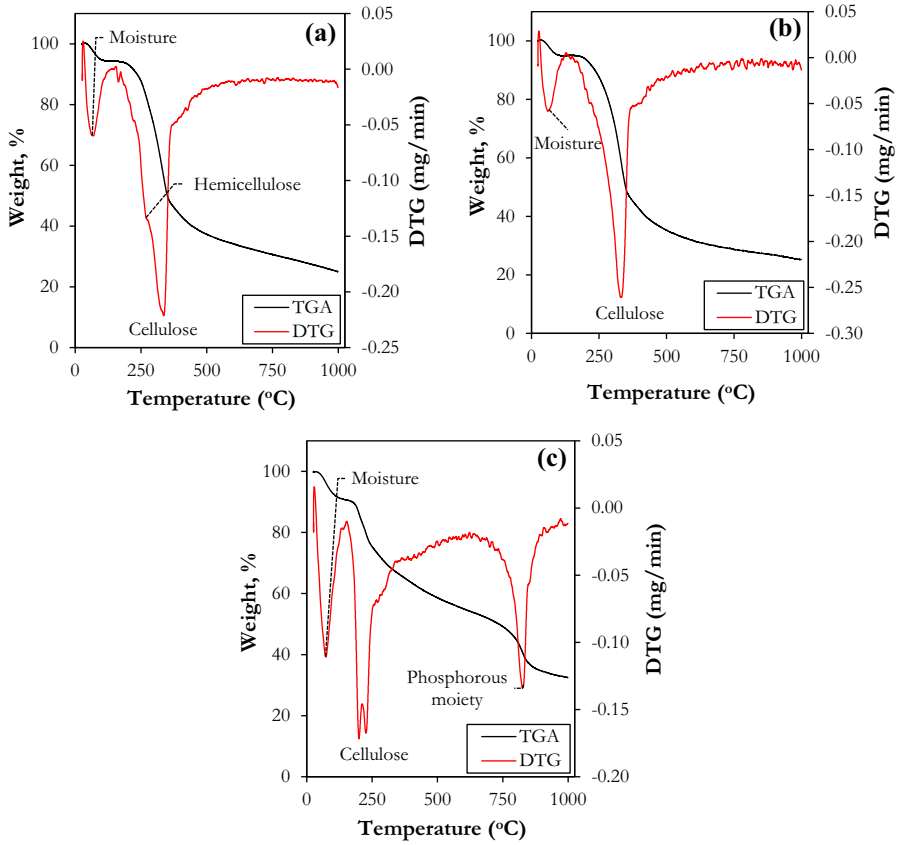

Fig. 4 Thermal profiles of **a** pristine, **b** NaOH treated **c** phosphorylated functional hazelnut shell waste

Lithium sorption performance of the biosorbent

The effect of biosorbent dosage

The sorbent dosage is of great importance with respect to the sorption studies as it determines the potential of material to uptake metal ions for a given initial concentration of the sorbent (Panda et al. 2011). The effect of biosorbent dosage is presented in Fig. 5a. Experimental results revealed that the percentage of sorption increased with increase in biosorbent dosages. This was in fact expected since increasing the biosorbent dosage provides greater surface area or higher sorption sites for a constant metal ion concentration. A maximum lithium sorption of 92% was achieved at biosorbent dosage of between 12 and 16 g/L and sorption for any biosorbent dosage beyond it gave almost the same uptake. Therefore, the use of 14 g/L biosorbent dosage is justified for economic point of view for the recovery of lithium from aqueous solutions.

The effect of pH

The solution pH is one of the factors that must be considered in sorption studies, as it can affect the structure of sorbent depending on the functional group it carries (especially if weak base or weak acidic) (Çiçek et al. 2018). The data presented in Fig. 5b indicates the sorption efficiency of phosphorylated functional hazelnut shell waste from pH 2 to pH 8. Relatively lower sorption of Li (82.15%) was observed at pH 2 but sorption behavior was similar within the range pH 3–8 by around 92% of lithium sorption efficiency. Since the biosorbent contains phosphoric acid derived functional group *pKa* values are 2.16, 7.21 and 12.32. Therefore, at pH 2, the functional group of the sorbent tends to stay in the molecular form, thus sorption of lithium was relatively low. Nonetheless, when the pH of solution was increased from 2 to 8, the functional group of the sorbent ionized, and sorption of lithium was enhanced as the next *pKa* value is 7.21.On the other hand, point of zero charge (PZC) value of this biosorbent was also

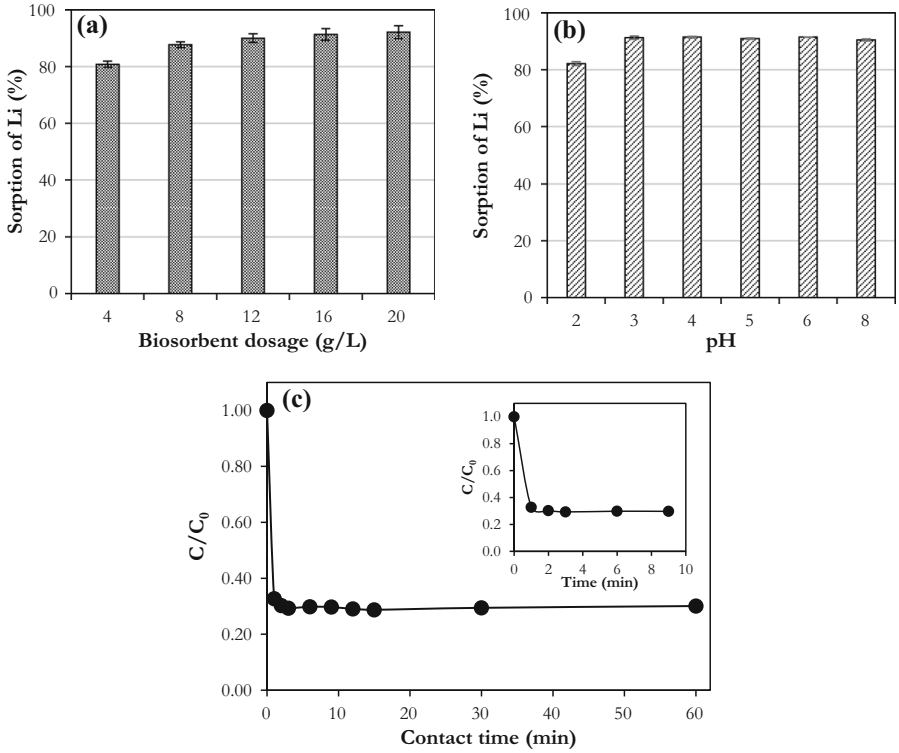

Fig. 5 **a** Effect of biosorbent dosage on lithium sorption efficiency (t: 24 h, C_0: 10 mg/L, pH 5–6, speed 180 rpm, T: 25 °C) **b** effect of solution pH on extent of lithium sorption (t: 24 h, biosorbent dosage: 14 g/L, C_0: 10 mg/L, pH 2–8, speed 180 rpm, T: 25 °C) **c** effect of contact time on lithium sorption on phosphorylated hazelnut shell waste (t: 0–60 min, biosorbent dosage: 12 g/L, C_0: 100 mg/L, pH 5–6, speed 180 rpm, T: 25 °C)

determined as 6.95 which means the biosorbent's surface was positively charged at solution pH below 6.95 resulting in the decrease of lithium sorption due to competition between lithium and protons ions for sorption active sites along with the repulsion of lithium ions. So, the lower the pH goes below pH_{PZC}, the greater the density of positive ions on the surface of phosphorylated functional hazelnut shell waste will be. As a result, except pH 2, no remarkable change was observed for the other pH values studied.

The effect of contact time

The effect of contact time on lithium sorption efficiency is depicted in Fig. 5c. As it is exhibited, sorption rate immediately increased, followed by a relatively slow process and then the optimal efficiency was reached within about 3 min. No obvious changes were observed from 3 to 60 min. Hence, the sorption process appeared to proceed very fast when the number of lithium ions to be transported from the medium are much larger than the numbers of available sites. This result also suggested that phosphorylated functional hazelnut shell waste has a high affinity toward lithium ions in aqueous solutions. On the other hand, it is truly surprising that the biosorbent possess a high lithium ions sorption efficiency, and reach sorption equilibrium quickly so that observable data could not be collected (i.e., sampling $< 1 min$ was highly difficult) in order to find related rate constants and rate determining step from proposed any of empirical models in the literature. In addition, cellulose based sorbents also reported in the literature performed quite rapid kinetics for different solutes (Arar 2019; Tomul et al. 2019; Xu et al. 2020; Zhang et al. 2020).

The effects of initial concentration and temperature

The effect of temperature dependence of lithium sorption by phosphorylated functional hazelnut shell waste with various initial ion concentration for different temperatures is presented in Fig. 6a. It is clearer for the solution having 100 mg/L initial lithium concentration that the equilibrium sorption capacity of phosphorylated hazelnut shell waste was considerably lower (4.97 mg/g) at the temperature of 45 °C than that at 35 °C (5.20 mg/g) and 25 °C

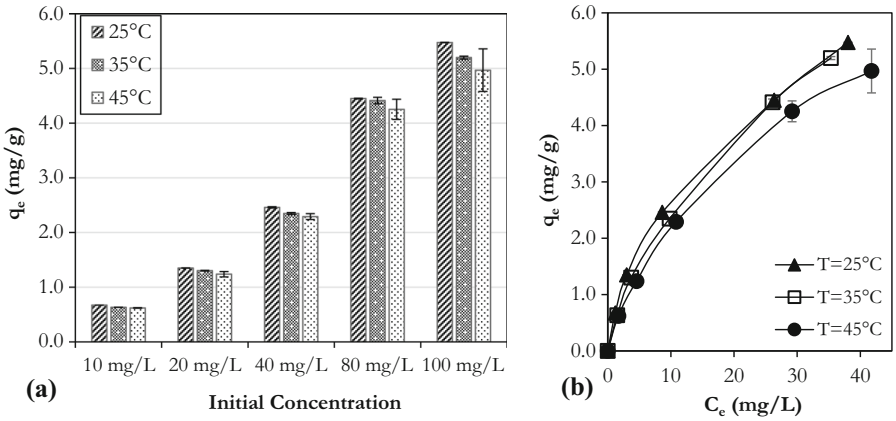

Fig. 6 **a** Effect of temperature on lithium uptake capacity of phosphorylated functional hazelnut shell waste at different initial concentrations **b** sorption isotherms of phosphorylated functional hazelnut shell waste (t: 24 h, biosorbent dosage: 14 g/L, C_0: 10–100 mg/L, pH 5–6, speed 180 rpm, T: 25–45 °C)

(5.48 mg/g). Since the equilibrium sorption capacity of the biosorbent decreased from 5.48 to 4.97 mg/g when the temperature was increased from 25 to 45 °C, it can be said that an exothermic reaction is controlling the sorption of lithium onto phosphorylated functional hazelnut shell in this temperature range. It can be attributed to high surface coverage depending on activation of reactive sites at lower temperature. On the other hand, the initial lithium concentration creates an important driving gradient force to overcome the mass transfer resistance to lithium ions between the aqueous and solid phases. The data for the lower temperature (25 °C) showed that lithium sorption capacity of phosphorylated hazelnut shell was increased from 0.67 to 5.48 mg/g with lithium concentration increasing from 10 to 100 mg/L due to a high driving force in terms of mass transfer, although the lithium percent sorption decreased from 92 to 67 due to the saturation of binding sites onto the biosorbent.

Sorption isotherms

The sorption isotherms of lithium onto phosphorylated functional hazelnut shell waste at different operation temperatures (25 °C, 35 °C and 45 °C) are given in Fig. 6b. According to the isotherm shape's classification, the biosorbent exhibited the F-type (Freundlich) isotherm, which is characterized by an indefinite multi-layer formation after completion of the monolayer and is found in sorbents with a wide distribution of pore sizes. Near to the point of inflexion a monolayer is completed, following which sorption occurs in successive layers (Ruthven 1984). As noted earlier, the process of lithium sorption onto the biosorbent occurred favorably at low solution temperature and high solution concentration.

Table 3 provides the corresponding parameters of the investigated sorption isotherms that were determined by the help of MATLAB® Software from the nonlinear regression technique. The correlation coefficient (R^2) and sum of squares of error (SSE) revealed that the experimental data of sorption equilibrium were satisfactorily described by the Freundlich model (0.996–0.999 and 0.0175–0.0607) than the Langmuir (0.991–0.998 and 0.0232–0.1572) and Temkin (0.953–0.959 and 0.6367–0.7221) models, respectively.

According to Langmuir model Q_{max} seems to increase first from 7.71 to 8.71 mg/g and then decrease to 8.04 mg/g as temperature increased from 25 to 45 °C which is quite comparable with some reported sorbents for lithium in Table 4. Although the nature of sorption is exothermic, this fluctuation may be stem from relatively lower model fitting compared to expected fitting for Freundlich model. However, decrease in the K_L value from 0.0579 to 0.0385 L/mg as temperature increased clarifies that binding affinity of the biosorbent to lithium ions in the solution was reduced as temperature was raised. This finding also justified that the contribution of pore filling to the sorption mechanism was not as substantial as the other surface interactions, such as hydrogen bonding and electrostatic attraction. For the Freundlich model, larger value of n_F (smaller value of $1/n_F$) implies stronger interaction between sorbent and solute. The values of $0.1 < (1/n_F) < 1.0$ for all temperatures shows that sorption of lithium is favorable (Ruthven

Table 3 Parameters of the sorption isotherm lithium onto phosphorylated functional hazelnut shell waste

Model	25 °C	35 °C	45 °C
Langmuir	$Q_{max} = 7.71 mg/g$	$Q_{max} = 8.71 mg/g$	$Q_{max} = 8.04 mg/g$
	$K_L = 0.0579 L/mg$	$K_L = 0.0406 L/mg$	$K_L = 0.0385 L/mg$
	$R^2 = 0.991$	$R^2 = 0.996$	$R^2 = 0.998$
	$SSE = 0.1572$	$SSE = 0.0685$	$SSE = 0.0232$
Freundlich	$K_F = 0.7129 mg/g(L/mg)^{1/n_F}$	$K_F = 0.5553 mg/g(L/mg)^{1/n_F}$	$K_F = 0.5176 mg/g(L/mg)^{1/n_F}$
	$n_F = 1.7834$	$n_F = 1.6321$	$n_F = 1.5861$
	$R^2 = 0.999$	$R^2 = 0.999$	$R^2 = 0.996$
	$SSE = 0.0204$	$SSE = 0.0175$	$SSE = 0.0607$
Temkin	$A = 1.0237 L/g$	$A = 0.7702 L/g$	$A = 0.6781 L/g$
	$B = 1.3761 J/mol$	$B = 1.4575 J/mol$	$B = 1.3943 J/mol$
	$R^2 = 0.959$	$R^2 = 0.953$	$R^2 = 0.955$
	$SSE = 0.6759$	$SSE = 0.7221$	$SSE = 0.6367$

Table 4 Comparison of sorption capacity of phosphorylated hazelnut shell waste with some published sorbents for lithium

Sorbent	Functional group	Maximum sorption capacity ($mg.g^{-1}$)	References
HMO-modified cellulose film	Hydrogen manganese oxide	21.6	(Tang et al. 2020)
Arthrospira platensis biomass	OH, –COOH, –NH, $–NH_2$, and $–NH_3$	1.75	(Zinicovscaia et al. 2020)
Cellulose microsphere adsorbent with sulfonic acid groups (CGS)	Sulfonic acid	16.0	(Xu et al. 2020)
Cellulose-based microsphere containing crown ethers groups (MCM-g-AB15C5)	4'-aminobenzo-15-crown-5 (AB15C5)	12.9	(Chen et al. 2019)
Lewatit TP 260 chelating resin	Aminomethylphosphonic acid	13.65	(Çiçek et al. 2018)
Magnetic lithium ion-imprinted polymer (Fe_3O_4@SiO_2@IIP)	2-(allyloxy) methyl-12-crown-4	4.07	(Luo et al. 2015)
Macroporous cellulose gel beads-based hybrid-type ion-exchanger (HIE)	Microcrystalline λ-MnO_2	9.72	(Sagara et al. 1989)
Phosphorylated hazelnut shell waste	Phosphorous group	7.71	This work

1984). Besides, Temkin isotherm considers explicitly the sorbent–solute interactions by a factor. Due to these interactions, the heat of sorption of all the molecules in the layer decreases linearly as coverage increases (Hameed et al. 2008).

Sorption thermodynamics

Thermodynamic parameters (ΔG°, ΔH° and ΔS°) of the lithium sorption can be essentially predicted by using following equation and van't Hoff approach, respectively:

$$\Delta G^\circ = -RTlnK_e \tag{7}$$

$$lnK_e = -\frac{\Delta H^\circ}{RT} + \frac{\Delta S^\circ}{R} \tag{8}$$

where ΔG° is Gibbs free energy change (kJ/mol), ΔH° is enthalpy change (kJ/mol) and ΔS° is entropy change (kJ/mol.K). Equilibrium constant (K_e, dimensionless)

can be obtained from the modification of Freundlich constant ($K_F, mg/g(L/mg)^{1/n_F}$), related with the thermodynamics of heterogeneous sorption, by the equation given below (Tran et al. 2016):

$$K_e = K_F \rho \left(\frac{10^6}{\rho}\right)^{\left(1-\frac{1}{n_F}\right)} \quad (9)$$

where ρ (g/mL) is the density of the aqueous solution but it can be simply approximated to density of water at the temperature of interest.

Thermodynamic parameters for the sorption of lithium by phosphorylated functional hazelnut shell waste were listed in Table S2. Gibbs free energy change, the basic principle for sorption spontaneity, must be negative for a feasible adsorption to occur so that negative ΔG° values confirm spontaneity of the sorption of lithium ions on biosorbent. Meanwhile, an increase in temperature caused less favorable sorption condition since greater (less negative) ΔG° values obtained at higher temperatures. This can also be supported by the exothermic nature of the sorption corresponding to the negative ΔH° value (− 51.07 kJ/mol). In addition, negative ΔS° value (− 0.125 kJ/kmol.K) indicated that the lithium sorption onto phosphorylated functional hazelnut shell become less random at the solid/solution interface during the sorption process. Another helpful outcome of the thermodynamic analysis is to estimate the physical nature of the ion sorption on the biosorbent. As an order of magnitude, ΔG° is in the range of 0 to − 20 kJ/mol for physical sorption and in the range of − 80 to − 400 kJ/mol for chemisorption (Salehi et al. 2012). Therefore, the mechanism of lithium sorption on phosphorylated functional hazelnut shell waste can be described as physical sorption based on ΔG° values that lie between 0 and − 20 kJ/mol. Most likely, rather than chemical bonds, weak physical electrostatic and van der Waals interactions attached lithium ions to the functional vacant sites of the biosorbent.

The effect of competitive ions

The effect of competitive ions was investigated in the existence of both other similar cations such as Na^+ and K^+ and Ca^{2+} and Mg^{2+} in the aqueous solution. As illustrated in Fig. 7a., these ions competed with Li^+ for the same sorption sites, therefore apparently the coexistence of the ions inhibited lithium sorption efficiency. Even though the presence of other cations in the solution simultaneously reduced slightly the separation efficiency of lithium from 92 to 85.54% when solution contains only lithium under the same conditions, overall sorption capacity of the phosphorylated functional hazelnut shell was improved. So that, Na^+, K^+, Ca^{2+} and Mg^{2+} separation percentages were also obtained as 58.47% 76.72%, 91.53% and 98.87%, respectively. This phenomenon is due to a shift in the equilibrium toward the formation of sorbent-solute complex with raising concentration of solute. On the other hand, the results showed that Ca^{2+} and Mg^{2+} highly competed with monovalent ions since they have higher valence and atomic radius as expected but the material still possessed a considerable lithium uptake capacity.

Moreover, as a preliminary study, this biosorbent was also tested with a geothermal water sample obtained from a well located in Seferihisar, İzmir region of which some physicochemical properties are given in Table S3 to check its lithium uptake performance in a real medium. As seen in Fig. 7b, lithium sorption efficiency decreased from 90 to 50% at optimum sorbent dosage when used in geothermal water compared to Li aqueous solution as expected. However, such performance comparison does not give precise idea since sorption efficiency is also highly dependent on initial Li concentration along with other competitor ions. Here in this preliminary test, the lithium concentration of the geothermal water used is 7.13 ppm and it also contains other quite high concentration of other ions, but the model solution contains only 10 ppm of Li. Despite relatively lower lithium sorption efficiency, the material proved its lithium capability in a real brine. By further modification of the material or applying pretreatment such as softening by hybrid methods the lithium sorption efficiency of this biosorbent can be improved and the research on this issue is going on and will be published in future.

Desorption of lithium and regeneration the biosorbent

The desorption study is of great importance to recycle the sorbent and to recover the lithium simultaneously. As depicted in Fig. 7c, according to desorption experiments conducted with NaCl, HCl and H_2SO_4,

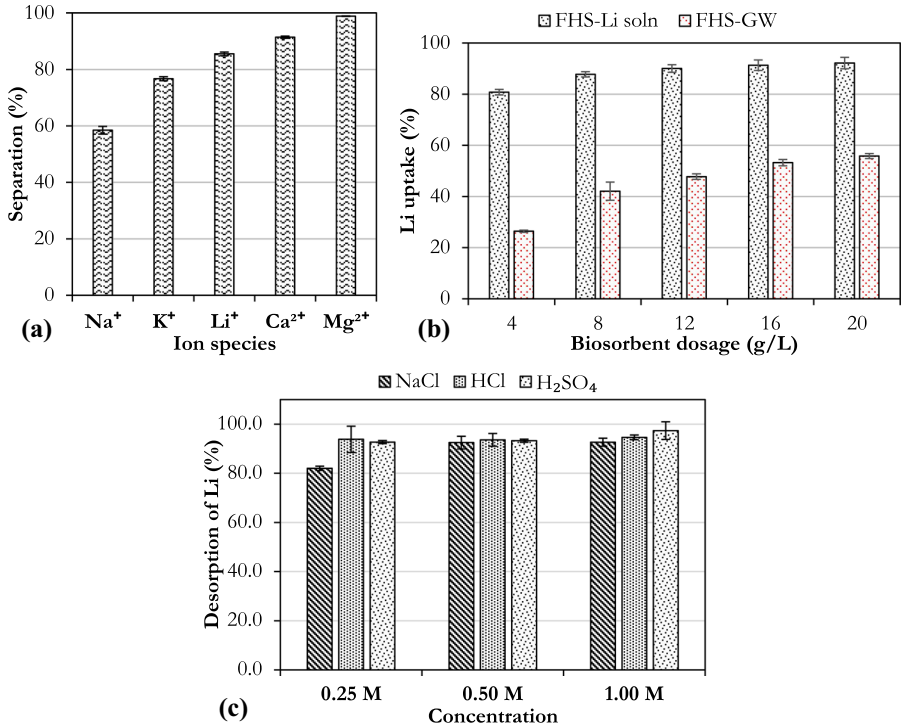

Fig. 7 **a** Effect of competitive ions on lithium sorption by phosphorylated functional hazelnut shell waste (t: 24 h, biosorbent dosage: 14 g/L, C_0: 10 mg/L for all species, pH 5–6, speed 180 rpm, T: 25 °C) **b** comparison of lithium uptake percentage by phosphorylated hazelnut shell waste (FHS) at different biosorbent dosage both in Li solution (Li-soln) and real geothermal water (GW) **c** comparison of desorption efficiency for phosphorylated functional hazelnut shell waste (t: 24 h, speed 180 rpm, T: 25 °C)

it was observed that the desorption ratio of lithium with 0.25 M NaCl was the lowest by 82% but this value was 93.8% and 92.7% for 0.25 M HCl and H_2SO_4, respectively. In contrast, for both 0.5 M and 1.0 M NaCl regenerant solution almost 93% desorption was recorded. Although the highest desorption efficiency was obtained with 1.0 M H_2SO_4 by 97.4%, using 1.0 M HCl resulted in considerable desorption ratio by 94.6%. In general, these results indicated that elution of lithium and regeneration of the biosorbent can easily be done using either of solutions at appropriate concentrations.

Conclusions and future perspectives

In the buildup of sustainable separation technologies for the recovery of valuable metals such as lithium, biosorption can be a facile route. A breakthrough in sorbents development is needed to solve the critical problem of recovery of strategic metal ions to promote circular (bio) economy. In this study, by applying recycling based (bio) technologies to recover valuable materials approach a novel biosorbent was developed from hazelnut shell wastes by grafting phosphorous functional groups. Characterization studies showed that hazelnut shell waste was functionalized by phosphorylation reaction successfully. Optimum sorbent dose was found to be 14 g/L. Thermodynamic analysis revealed that the sorption of lithium on phosphorylated functional hazelnut shell waste was spontaneous, exothermic, and more random. As temperature increased sorption of lithium decreased due to exothermic nature of the biosorbent which is advantageous for metal recovery. Although as initial concentration increased sorption of lithium enhanced, no considerable effect is observed for the solution pH except pH 2. Sorption behavior of phosphorylated functional hazelnut shell waste was well described by Freundlich isotherm, but maximum sorption of lithium was estimated as 7.71 mg/g at 25 °C by Langmuir model. The rate of sorption was quite rapid therefore

kinetic trials were out of range in terms of duration which can be one of superior properties of this biosorbent. Even though coexistence of other cations such as Na^+, K^+, Ca^{2+} and Mg^{2+} in the solution reduced slightly sorption efficiency of Li from 92 to 85.54% under the same condition when only Li^+ exists, the biosorbent still exhibited a considerable lithium capability. Moreover, the Li loaded phosphorylated functional hazelnut shell waste can easily be regenerated with 1.0 M HCl or H_2SO_4 with high desorption efficiencies. It can be concluded through experimental results for its significant and fast lithium sorption capacity, low-cost and easily obtained properties, phosphorylated hazelnut shell waste could be considered a promising sorbent for lithium recovery from natural sources such as geothermal water for which a preliminary study was performed. By doing this, goals of the conversion of an abundant waste, a renewable raw material, into value-added products and the recovery of valuable minerals to promote renewable energy will be met simultaneously. However, since the biosorbent is at very early stage of its development, a further modification step for either the material or the biosorption process is under consideration to increase its lithium sorption efficiency. Since the phosphorylated biosorbent can be used in the forms of proton as counterions if the solution is alkaline or it can be used in the forms of sodium as counterions if the solution is acidic. On the other hand, chromatographic separation of Li from aqueous solutions will be carried out by crosslinked phosphorylated biosorbent and will be published in the literature available to the general public.

Acknowledgments The authors greatly acknowledge Assoc. Prof. Dr. Özgür Arar at Ege University, Department of Chemistry for his kind support. In addition, we would like to thank "Center for Materials Research" for characterization analyses and "Environmental Research and Development Center" for ICP-OES analyses at Izmir Institute of Technology Integrated Research Center.

Funding This study was financially supported through the project of The Scientific and Technological Research Council of Turkey-TUBITAK (Project No. 219M219).

Declarations

Conflict of interest The authors declare that they have no competing financial interest associated with the work presented. Additionally, the authors assure that there is no conflict of interest.

Ethical approval Authors guarantee that this research paper is original and has not been previously published, in whole or in part, and that is not under consideration by another journal.

Human participants The study does not include animal studies or human participants.

References

Alasalvar C, Amaral JS, Satır G, Shahidi F (2009) Lipid characteristics and essential minerals of native Turkish hazelnut varieties (*Corylus avellana* L.). Food Chem 113:919–925

Alkaya E, Erguder TH, Demirer GN (2010) Effect of operational parameters on anaerobic co-digestion of dairy cattle manure and agricultural residues: a case study for the Kahramanmaraş region in Turkey. Eng Life Sci 10:552–559

Aoki D, Nishio Y (2010) Phosphorylated cellulose propionate derivatives as thermoplastic flame resistant/retardant materials: Influence of regioselective phosphorylation on their thermal degradation behaviour. Cellulose 17:963–976. https://doi.org/10.1007/s10570-010-9440-8

Arar Ö (2019) Preparation of anion-exchange cellulose for the removal of chromate. J Chil Chem Soc 64:4471–4474

Cagnon B, Py X, Guillot A et al (2009) Contributions of hemicellulose, cellulose and lignin to the mass and the porous properties of chars and steam activated carbons from various lignocellulosic precursors. Bioresour Technol 100:292–298

Chen I, Xu C, Peng J et al (2019) Novel functionalized cellulose microspheres for efficient separation of lithium ion and its isotopes: synthesis and adsorption performance. Molecules 24:2762

Chuah TG, Jumasiah A, Azni I et al (2005) Rice husk as a potentially low-cost biosorbent for heavy metal and dye removal: an overview. Desalination 175:305–316

Çiçek A, Yilmaz O, Arar Ö (2018) Removal of lithium from water by aminomethylphosphonic acid-containing resin. J Serbian Chem Soc 83:1059–1069. https://doi.org/10.2298/JSC170930020C

Çöpür Y, Güler C, Taşçıoğlu C, Tozluoğlu A (2008) Incorporation of hazelnut shell and husk in MDF production. Bioresour Technol 99:7402–7406

Costes L, Laoutid F, Khelifa F et al (2016) Cellulose/phosphorus combinations for sustainable fire retarded polylactide. Eur Polym J 74:218–228

Das K, Ray D, Bandyopadhyay NR, Sengupta S (2010) Study of the properties of microcrystalline cellulose particles from different renewable resources by XRD, FTIR, nanoindentation, TGA and SEM. J Polym Environ 18:355–363

Fomina M, Gadd GM (2014) Biosorption: current perspectives on concept, definition and application. Bioresour Technol 160:3–14

French AD (2014) Idealized powder diffraction patterns for cellulose polymorphs. Cellulose 21:885–896

French AD (2020) Increment in evolution of cellulose crystallinity analysis. Cellulose 27:5445–5448. https://doi.org/10.1007/s10570-020-03172-z

French AD, Santiago Cintrón M (2013) Cellulose polymorphy, crystallite size, and the Segal Crystallinity Index. Cellulose 20:583–588. https://doi.org/10.1007/s10570-012-9833-y

Freundlich H (1907) Über die adsorption in lösungen. Zeitschrift Für Phys Chemie 57:385–470

Ghanadpour M, Carosio F, Larsson PT, Wågberg L (2015) Phosphorylated cellulose nanofibrils: a renewable nanomaterial for the preparation of intrinsically flame-retardant materials. Biomacromol 16:3399–3410

Gozaydin G, Yuksel A (2017) Valorization of hazelnut shell waste in hot compressed water. Fuel Process Technol 166:96–106

Grosjean C, Miranda PH, Perrin M, Poggi P (2012) Assessment of world lithium resources and consequences of their geographic distribution on the expected development of the electric vehicle industry. Renew Sustain Energy Rev 16:1735–1744

Guney MS (2013) Utilization of hazelnut husk as biomass. Sustain Energy Technol Assessments 4:72–77

Hameed BH, Tan IAW, Ahmad AL (2008) Adsorption isotherm, kinetic modeling and mechanism of 2,4,6-trichlorophenol on coconut husk-based activated carbon. Chem Eng J 144:235–244. https://doi.org/10.1016/j.cej.2008.01.028

Hoşgün EZ, Bozan B (2019) Effect of different types of thermochemical pretreatment on the enzymatic hydrolysis and the composition of hazelnut shells. Waste Biomass Valorization 11:3739–3748

Illy N, Fache M, Ménard R et al (2015) Phosphorylation of bio-based compounds: the state of the art. Polym Chem 6:6257–6291. https://doi.org/10.1039/c5py00812c

Inagaki N, Nakamura S, Asai H, Katsuura K (1976) Phosphorylation of cellulose with phosphorous acid and thermal degradation of the product. J Appl Polym Sci 20:2829–2836

Kim JS, Lee YY, Kim TH (2016) A review on alkaline pretreatment technology for bioconversion of lignocellulosic biomass. Bioresour Technol 199:42–48

Kim S, Joo H, Moon T et al (2019) Rapid and selective lithium recovery from desalination brine using an electrochemical system. Environ Sci Process Impacts 21:667–676

Kitajou A, Suzuka Y, Nishihama S et al (2006) Development of λ-MnO2 adsorbent toward the practical recovery of lithium from seawater. J Ion Exch 17:7–13

Kokol V, Božič M, Vogrinčič R, Mathew AP (2015) Characterisation and properties of homo-and heterogenously phosphorylated nanocellulose. Carbohydr Polym 125:301–313

Langmuir I (1916) The constitution and fundamental properties of solids and liquids. Part I. Solids J Am Chem Soc 38:2221–2295

Luneva NK, Ezovitova TI (2014) Cellulose phosphorylation with a mixture of orthophosphoric acid and ammonium polyphosphate in urea medium. Russ J Appl Chem 87:1558–1565. https://doi.org/10.1134/S1070427214100243

Luo X, Guo B, Luo J et al (2015) Recovery of lithium from wastewater using development of Li ion-imprinted polymers. ACS Sustain Chem Eng 3:460–467

Moubarik A, Grimi N (2015) Valorization of olive stone and sugar cane bagasse by-products as biosorbents for the removal of cadmium from aqueous solution. Food Res Int 73:169–175

Ngo HH, Guo W, Zhang J et al (2015) Typical low cost biosorbents for adsorptive removal of specific organic pollutants from water. Bioresour Technol 182:353–363

Özlem T (2019) Potential use of hazelnut processing plant wastes as a sorbent for the simultaneous removal of multi-elements from water. Mühendislik Bilim Ve Tasarım Derg 7:301–312

Panda L, Das B, Rao DS, Mishra BK (2011) Application of dolochar in the removal of cadmium and hexavalent chromium ions from aqueous solutions. J Hazard Mater 192:822–831

Park J, Sato H, Nishihama S, Yoshizuka K (2012) Lithium recovery from geothermal water by combined adsorption methods. Solvent Extr Ion Exch 30:398–404. https://doi.org/10.1080/07366299.2012.687165

Poletto M, Zattera AJ, Forte MMC, Santana RMC (2012) Thermal decomposition of wood: influence of wood components and cellulose crystallite size. Bioresour Technol 109:148–153

Recepoğlu YK, Kabay N, Yılmaz-Ipek İ et al (2017) Equilibrium and kinetic studies on lithium adsorption from geothermal water by λ-MnO2. Solvent Extr Ion Exch 35:221–231. https://doi.org/10.1080/07366299.2017.1319235

Recepoğlu YK, Kabay N, Yoshizuka K et al (2018) Effect of operational conditions on separation of lithium from geothermal water by λ-MnO2 using ion exchange-membrane filtration hybrid process. Solvent Extr Ion Exch 36:499–512. https://doi.org/10.1080/07366299.2018.1529232

Rol F, Belgacem N, Meyer V et al (2019) Production of fire-retardant phosphorylated cellulose fibrils by twin-screw extrusion with low energy consumption. Cellulose 26:5635–5651

Romero-Cano LA, Gonzalez-Gutierrez LV, Baldenegro-Perez LA (2016) Biosorbents prepared from orange peels using Instant Controlled Pressure Drop for Cu (II) and phenol removal. Ind Crops Prod 84:344–349

Ruthven DM (1984) Principles of adsorption and adsorption processes. John Wiley & Sons

Sagara F, Ning WB, Yoshida I, Ueno K (1989) Preparation and adsorption properties of λ-MnO2-cellulose hybrid-type lon-exchanger for lithium ion. Application to the enrichment of lithium ion from seawater. Sep Sci Technol 24:1227–1243

Salehi E, Madaeni SS, Vatanpour V (2012) Thermodynamic investigation and mathematical modeling of ion-imprinted membrane adsorption. J Memb Sci 389:334–342

Sarker TC, Azam SMGG, El-Gawad AMA et al (2017) Sugarcane bagasse: a potential low-cost biosorbent for the removal of hazardous materials. Clean Technol Environ Policy 19:2343–2362

Segal L, Creely JJ, Martin AE Jr, Conrad CM (1959) An empirical method for estimating the degree of crystallinity

of native cellulose using the X-ray diffractometer. Text Res J 29:786–794
Segovia-Sandoval SJ, Ocampo-Pérez R, Berber-Mendoza MS et al (2018) Walnut shell treated with citric acid and its application as biosorbent in the removal of Zn (II). J Water Process Eng 25:45–53
Şenol H (2019) Biogas potential of hazelnut shells and hazelnut wastes in Giresun City. Biotechnol Reports. https://doi.org/10.1016/j.btre.2019.e00361
Shi Y, Belosinschi D, Brouillette F et al (2014) Phosphorylation of Kraft fibers with phosphate esters. Carbohydr Polym 106:121–127
Socrates G (2004) Infrared and Raman characteristic group frequencies: tables and charts. John Wiley & Sons
Suflet DM, Chitanu GC, Popa VI (2006) Phosphorylation of polysaccharides: new results on synthesis and characterisation of phosphorylated cellulose. React Funct Polym 66:1240–1249. https://doi.org/10.1016/j.reactfunctpolym.2006.03.006
Tang L, Huang S, Wang Y et al (2020) Highly efficient, stable, and recyclable hydrogen manganese oxide/cellulose film for the extraction of lithium from seawater. ACS Appl Mater Interfaces 12:9775–9781
Tempkin MI, Pyzhev V (1940) Kinetics of ammonia synthesis on promoted iron catalyst. Acta Phys Chim USSR 12:327
Tomul F, Arslan Y, Başoğlu FT et al (2019) Efficient removal of anti-inflammatory from solution by Fe-containing activated carbon: Adsorption kinetics, isotherms, and thermodynamics. J Environ Manage 238:296–306
Tran HN, You S-J, Chao H-P (2016) Thermodynamic parameters of cadmium adsorption onto orange peel calculated from various methods: a comparison study. J Environ Chem Eng 4:2671–2682
Tran HN, You S-J, Nguyen TV, Chao H-P (2017) Insight into the adsorption mechanism of cationic dye onto biosorbents derived from agricultural wastes. Chem Eng Commun 204:1020–1036
Wang S, Li P, Zhang X et al (2017) Selective adsorption of lithium from high Mg-containing brines using HxTiO3 ion sieve. Hydrometallurgy 174:21–28
Wang S, Chen X, Zhang Y et al (2018) Lithium adsorption from brine by iron-doped titanium lithium ion sieves. Particuology 41:40–47
Witek-Krowiak A, Szafran RG, Modelski S (2011) Biosorption of heavy metals from aqueous solutions onto peanut shell as a low-cost biosorbent. Desalination 265:126–134
Xu X, Gao Y, Gao B et al (2011) Characteristics of diethylenetriamine-crosslinked cotton stalk/wheat stalk and their biosorption capacities for phosphate. J Hazard Mater 192:1690–1696
Xu N, Li S, Guo M et al (2019) Synthesis of H4Mn5O12 nanotubes lithium ion sieve and its adsorption properties for Li+ from aqueous solution. ChemistrySelect 4:9562–9569
Xu C, Yu T, Peng J et al (2020) Efficient adsorption performance of lithium ion onto cellulose microspheres with sulfonic acid groups. Quantum Beam Sci 4:6
Yabusaki K (2010) Cellulose II phosphate ester and metal-adsorbing material using the same. Patent US7803937B2
Yoshizuka K, Fukui K, Inoue K (2002) Selective recovery of lithium from seawater using a novel MnO2 type adsorbent. Ars Separatoria Acta 79–86
Zhang M, Yin Q, Ji X et al (2020) High and fast adsorption of cd (ii) and pb (ii) ions from aqueous solutions by a waste biomass based hydrogel. Sci Rep 10:1–13
Zinicovscaia I, Yushin N, Pantelica A et al (2020) Lithium biosorption by Arthrospira (Spirulina) platensis biomass. Ecol Chem Eng S 27:271–280